Probabilities of moderately atypical fluctuations of the size of a swarm of Brownian bees

Pavel Sasorov,[1,*] Arkady Vilenkin,[2,†] and Naftali R. Smith[3,‡]
[1]*Institute of Physics CAS, ELI Beamlines, 182 21 Prague, Czech Republic*
[2]*Racah Institute of Physics, Hebrew University of Jerusalem, Jerusalem 91904, Israel*
[3]*Department of Solar Energy and Environmental Physics, Blaustein Institutes for Desert Research, Ben-Gurion University of the Negev, Sede Boqer, 8499000, Israel*

(Received 15 September 2022; accepted 17 January 2023; published 30 January 2023)

The "Brownian bees" model describes an ensemble of $N = \text{const}$ independent branching Brownian particles. The conservation of N is provided by a modified branching process. When a particle branches into two particles, the particle which is farthest from the origin is eliminated simultaneously. The spatial density of the particles is governed by the solution of a free boundary problem for a reaction-diffusion equation in the limit of $N \gg 1$. At long times, the particle density approaches a spherically symmetric steady-state solution with a compact support of radius $\bar{\ell}_0$. However, at finite N, the radius of this support, L, fluctuates. The variance of these fluctuations appears to exhibit a logarithmic anomaly [Siboni *et al.*, Phys. Rev. E **104**, 054131 (2021)]. It is proportional to $N^{-1} \ln N$ at $N \to \infty$. We investigate here the tails of the probability density function (PDF), $P(L)$, of the swarm radius, when the absolute value of the radius fluctuation $\Delta L = L - \bar{\ell}_0$ is sufficiently larger than the typical fluctuations' scale determined by the variance. For negative deviations the PDF can be obtained in the framework of the optimal fluctuation method. This part of the PDF displays the scaling behavior $\ln P \propto -N\Delta L^2 \ln^{-1}(\Delta L^{-2})$, demonstrating a logarithmic anomaly at small negative ΔL. For the opposite sign of the fluctuation, $\Delta L > 0$, the PDF can be obtained with an approximation of a single particle, running away. We find that $\ln P \propto -N^{1/2}\Delta L$. We consider in this paper only the case when $|\Delta L|$ is much less than the typical radius of the swarm at $N \gg 1$.

DOI: 10.1103/PhysRevE.107.014140

I. INTRODUCTION

We continue in this paper investigations of a model of nonequilibrium statistical physics, which is known under the name "Brownian bees" [1–4]. This model combines two important fields of statistical physics: branching Brownian motion (BBM) and nonequilibrium steady states (NESSs). BBM includes two processes: Brownian motion together with a branching process. Growing ensembles described by this model have been investigated for a long time. See, for example, Refs. [5,6] and more recent Refs. [7–10]. In its turn, ensembles of reacting and diffusing particles, representing NESSs, are important for description of many natural systems. Their investigations occupy a very distinguishable area in nonequilibrium statistical mechanics [11–15].

The "Brownian bees" model represents a system whose dynamics are irreversible in time, based on the branching Brownian dynamics of N particles (bees). Conservation of their total number is provided by removing the bee that is farthest from the origin at the moment of any branching. The removing causes nonlocal interaction between bees and destroys time reversibility of the system even in its steady state. Choosing proper units for time and distance we may set that the diffusion coefficient for the Brownian motion and rate of branching of each bee are equal to 1. Most of this paper is devoted to the one-dimensional (1D) case at $N \to \infty$.

It has been shown [1] that at any finite time t a coarse-grained density distribution $u(x,t)$ of the bees, normalized by N, obeys the following mean field theory at $N \to \infty$:

$$\partial_t u(x,t) = \partial_x^2 u(x,t) + u(x,t), \quad |x| \leqslant \bar{\ell}(t), \tag{1}$$

$$u(x,t) = 0, \quad |x| > \bar{\ell}(t), \tag{2}$$

$$\int_{-\bar{\ell}(t)}^{\bar{\ell}(t)} u(x,t)\,dx = 1. \tag{3}$$

As one can see, the compact support of $u(x,t)$, at all finite $t > 0$, is centered at the origin. Effectively, there are two absorbing walls, at $x = \pm\bar{\ell}(t)$, which move in synchrony so as to keep the number of particles constant at all times. In Ref. [1] it is shown that fluctuations of the coarse-grained density around $u(x,t)$ tend to 0 at $N \to \infty$.

It has been proved also [2] that the solution $u(x,t)$ of the system (1)–(3) tends at $t \to \infty$ to the following steady state:

$$U(x) = \begin{cases} \frac{1}{2}\cos x, & |x| \leqslant \bar{\ell}_0, \\ 0, & |x| > \bar{\ell}_0, \end{cases} \tag{4}$$

where $\bar{\ell}_0 = \pi/2$ and $\bar{\ell}(t) \to \bar{\ell}_0$ at $t \to \infty$.

We consider in this paper small relative fluctuations of the swarm radius $L = \max_{i\in\{1,\ldots,N\}} x_i$, where $x_1, \ldots, x_N$ are the positions of the particles, in the steady state described by Eq. (4). Consideration of this problem started in Refs. [3,4].

*pavel.sasorov@gmail.com
†vilenkin@mail.huji.ac.il
‡naftalismith@gmail.com

Monte Carlo simulations of the original microscopic model and analytic investigation of a Langevin equation that describes typical fluctuations in this model gave the following expression [4] for the variance of L at the steady state at $N \to \infty$:

$$\operatorname{var} L \simeq \frac{2}{\pi}\frac{\ln N}{N}. \tag{5}$$

This result was obtained in Ref. [4] by linearization of the Langevin equation; and the logarithmic anomaly results from a truncation of a formally divergent analytic expression for $\operatorname{var} L$. This anomaly originates from the fact that fluctuations of the particle density at all spatial scales give contributions that are of the same order of magnitude to the fluctuations of L.

The "Brownian bees" model belongs to a broader class of N-particle branching Brownian models with selection (NBBM). It was introduced initially in Refs. [16,17]. A lot of works investigating this class of models are cited in Ref. [4]. It is interesting that many NBBM systems expose logarithmic anomalies in the statistical behavior of the edge particles. This is an additional motivation for studies of the Brownian bees model.

In this paper we present results of our investigation of the tails of the probability density function (PDF) of instantaneous values of L at the steady state, $P(L)$. We consider moderately large fluctuations, $\Delta L = L - \ell_0$, which on the one hand are much larger than the typical fluctuations' scale, $|\Delta L| \gg \sigma(L) = \sqrt{\operatorname{var} L}$, but, on the other hand, are relatively small fluctuations in the sense that $|\Delta L| \ll 1$.

Let us briefly summarize our main findings, while describing the structure of the rest of the paper. For negative ΔL, the fluctuations involve many particles. So they can be considered in the framework of the optimal fluctuation method (OFM). The latter, known also under other names (the instanton method, the weak noise theory, and the macroscopic fluctuation theory), considers a single "trajectory" of coarse-grained density history, giving maximal contribution to the probability [11,12,18–23]. It is briefly recalled in Sec. II. Applying the OFM to the present problem in Sec. III, we obtain at $N \to \infty$:

$$-\ln P(L) = \frac{\pi}{4} N \frac{\Delta L^2}{|\ln \Delta L^2|} + \cdots. \tag{6}$$

This result is obtained by combining analytical and numerical methods. The nonanalytic structure of this expression at $-\Delta L \to 0$ provides a smooth matching of this result with the Gaussian distribution that describes typical fluctuations with mean $\bar{\ell}_0$ and variance (5). However, the presence of the logarithm in this asymptotic expression means that it can hardly be obtained by regular perturbation methods at $-\Delta L \ll 1$.

Atypically large positive fluctuations of L turn out to be dominated by the dynamical behavior of the single farthest particle. Analogous situations are encountered in many other problems of extreme value statistics [24]. This approach, applied in Sec. IV for the present problem, gives at $N \gg 1$:

$$-\ln P(L) = \sqrt{N}\,\Delta L + \cdots. \tag{7}$$

The result in this regime does not match smoothly with the typical fluctuations, Gaussian regime. We expect there to be a crossover between the two regimes which we do not attempt to analyze in the present work. Our main results for the distribution $P(L)$ are plotted schematically in Fig. 1. Finally, Sec. V is devoted to conclusions and discussions, including generalizations of our results to higher dimensions.

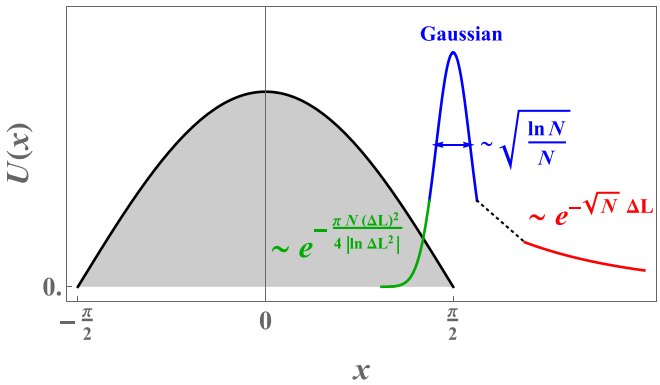

FIG. 1. A schematic plot of the distribution of the swarm radius, $P(L)$. The peak of the distribution is at $x = \pi/2$ which is the edge of the mean-field swarm density $U(x)$. Typical fluctuations are Gaussian with variance (5) [4], while the two, very asymmetric large deviation tails of $P(L)$ are described by Eqs. (6) and (7). The dotted line corresponds to a conjectured crossover regime between the typical fluctuations and the atypical positive fluctuations regime.

II. OPTIMAL FLUCTUATION METHOD: GOVERNING EQUATIONS

The OFM employs an idea that probability of transition between two states of a stochastic system is dominated by the probability of an "optimal" (most likely) trajectory. In our case this trajectory is given by $q(x,t)$: A coarse-grained normalized density history of the fluctuating swarm of Brownian bees. The designation $u(x,t)$ we reserve for particular trajectories, obeying the mean field system of equations (1)–(3) (without fluctuations). The most probable trajectory is defined by minimization of a functional of $q(x,t)$. Hence, this problem corresponds to the investigation of some classical field theory that can be recast as a Hamiltonian field theory. It involves, in addition to a generalized "coordinate" $q(x,t)$ a generalized "momentum" field $p(x,t)$. Before introducing the classical field theory corresponding to our present system, we may say that in a many-particle system, typically the OFM gives a correct evaluation of the probability for atypical fluctuations when they involve many particles.

The derivation of the OFM for the Brownian bees models was considered in detail together with references of previous publications in Ref. [3]. The process providing the conservation of total number of bees, N, in the swarm is introduced in the OFM system as a constraint and as boundary conditions at $|x| = L(t)$, whereas the fields $p(x,t)$ and $q(x,t)$ are defined only at $x \in [-L(t), L(t)]$. The density of the unconstrained Hamiltonian is defined as

$$\mathcal{H}_0(q,p) = (e^p - 1)q - (\partial_x q)(\partial_x p) + q(\partial_x p)^2, \tag{8}$$

whereas the unconstrained Hamiltonian is equal to

$$H_0[q(x),\, p(x)] = \int_{-L(t)}^{L(t)} \mathcal{H}_0(q,\, p)\, dx. \tag{9}$$

The constraint coming from conservation of the total number of bees

$$\int_{-L(t)}^{L(t)} q(x,t)\, dx = 1 \quad \text{for any } t \tag{10}$$

is introduced by means of a Lagrangian multiplier $\lambda(t)$, so that constrained Hamiltonian becomes

$$H[q(x),\, p(x),\, \lambda(t)] = H_0[q(x),\, p(x)] + \lambda(t) \int_{-L(t)}^{L(t)} q(x,t)\, dx. \tag{11}$$

It depends, in general, explicitly on time t. The density of the constrained Hamiltonian is

$$\mathcal{H}(q,\, p) = \mathcal{H}_0(q,\, p) + \lambda(t) q. \tag{12}$$

The fields $q(x,t)$ and $p(x,t)$ have support at $|x| < L(t)$, whereas the boundary conditions at the absorbing wall, $|x| = L(t)$, are

$$q(|x| = L(t), t) = p(|x| = L(t), t) = 0. \tag{13}$$

We assume that the system is allowed to evolve for a very long time prior to the time $t = 0$ at which the radius is measured. This leads to the following initial conditions:

$$q(x, t \to -\infty) = U(x)\,, \quad p(x, t \to -\infty) = 0, \tag{14}$$

and hence $L(t \to -\infty) = \bar{\ell}_0$. Trajectories of this Hamilton system, determined by the Hamilton equations

$$\partial_t q = \frac{\delta H}{\delta p} = q e^p + \boldsymbol{\nabla} \cdot (\boldsymbol{\nabla} q - 2 q \boldsymbol{\nabla} p), \tag{15}$$

$$\partial_t p = -\frac{\delta H}{\delta q} = -(e^p - 1) - \nabla^2 p - (\boldsymbol{\nabla} p)^2 - \lambda(t), \tag{16}$$

maximize locally the probability density, $\mathcal{P}[q(x,t)]$, at the trajectory $q(x,t)$ which is determined in the OFM framework by the action $S[q(x,t)]$ of an unconstrained mechanical system:

$$-N^{-1} \ln \mathcal{P}[q(x,t)] = S[q(x,t)], \tag{17}$$

where the action functional $S[q(x,t)]$ on an arbitrary trajectory $q(x,t)$ per particle is defined as

$$S[q(x,t)] = \int_{-\infty}^{0} dt \int_{-L(t)}^{L(t)} [p \partial_t q - \mathcal{H}_0]\, dx. \tag{18}$$

Here the momentum field p should obey Eq. (15) as usual and the boundary condition (13). Minimization of the action with respect to small variations $\delta q(x,t)$ of the trajectory $q(x,t)$ at $t < 0$ gives the second Hamilton equation (16). This minimization is necessary because the OFM implies the following evaluation of the probability that $L < \ell$ for $\ell < \bar{\ell}_0$:

$$-N^{-1} \ln \mathbb{P}\mathrm{rob}\,(L < \ell) \simeq \min_{L(0)=\ell} S[q(x,t)], \tag{19}$$

where the minimization is over histories of the density $q(x,t)$ and of the radius $L(t)$, conditioned on $L(0) = \ell$. It corresponds to Eq. (17) and to the following expression for the PDF, $P(L)$ [25]:

$$-N^{-1} \ln P(L) \simeq \min_{L(0)=\ell} S[q(x,t)], \tag{20}$$

where the minimization is over all possible trajectories $q(x,t)$ obeying the constraints.

The minimization, entering Eq. (20), means in particular minimization over the final density $q(x,0)$ of the particles inside the interval $|x| < L$ at $t = 0$. Requiring the variation of $S[q(x,t)]$ over $q(x,0)$ to vanish, conditioned on $\int q(x,0)\, dx = 1$, that is equivalent to $\int \delta q(x,0)\, dx = 0$, gives a boundary condition at $t = 0$. We may follow Ref. [26] to get analogously this boundary condition for the present problem. Consider two solutions of Eqs. (15) and (16) that are close to each other, $q(x,t)$ and $q(x,t) + \delta q(x,t)$, obeying the boundary conditions (14) at $t = -\infty$. Then we may write for the variation δS:

$$\delta S = \int_{-\infty}^{0} dt \int_{-L(t)}^{L(t)} \left[\delta p \partial_t q + p \partial_t \delta q - \frac{\partial \mathcal{H}_0}{\partial q} \delta q - \frac{\partial \mathcal{H}_0}{\partial p} \delta p\right] dx.$$

Using Eqs. (15) and (16), we obtain

$$\delta S = \int_{-\infty}^{0} dt \int_{-L(t)}^{L(t)} [\partial_t (p \delta q) + \lambda(t) \delta q]\, dx.$$

Applying the boundary condition (14) and the condition (10), we obtain

$$\delta S = \int_{-L(0)}^{L(0)} p(x,0) \delta q(x,0)\, dx.$$

For the optimal $q(x,t)$ the variation δS should vanish. Combining this requirement with the previous equation and with Eq. (10), we obtain that $\partial_x p(x,0) = 0$ and hence

$$p(x,0) = \Lambda = \text{const} \quad \text{for } |x| < L(0). \tag{21}$$

This relationship gives the last boundary condition in time t for our problem. For convenience, the formulation of the OFM problem is briefly summarized in Appendix A.

The OFM problem contains one constant Λ and two yet unknown functions $\lambda(t)$ and $L(t)$. The latter one defines also the constant $L(0)$. When the function $\lambda(t)$ is known and tends to 0 sufficiently fast at $t \to -\infty$, then the condition of solvability of the OFM problem determines Λ and $L(t)$ [and hence $L(0)$]. As a result, the solution of the OFM problem demonstrates a functional degree of freedom that is determined by the choice of $\lambda(t)$. Thus our action S is actually a functional of $\lambda(t)$: $S = S[\lambda(t)]$. An equation that follows from the condition of vanishing of variational derivative $\delta S[\lambda(t)]/\delta\lambda = 0$ under the constraint that $L(0) = \ell$ looks very cumbersome and almost useless. We will try in Sec. III to find an approximation to an optimal $\lambda(t)$ at $\Delta L = L(0) - \bar{\ell}_0 \to 0$ with another approach, that will give a leading order of the optimal action S in this limit. Note that we may not distinguish L and $L_0 = L(0)$ in the frame of the OFM. For the *locally* optimal at $t < 0$ trajectories, the general expression (18) for the action becomes simpler:

$$S = \int_{-\infty}^{0} dt \int_{-L(t)}^{L(t)} dx\, [q(p e^p - e^p + 1) + q(\partial_x p)^2]. \tag{22}$$

Integrating the first term in Eq. (18) by parts, and using Eq. (16), we obtain even simpler expression for the

action:

$$S = \Lambda + \int_{-\infty}^{0} \lambda(t)\, dt. \tag{23}$$

However, the latter expression is not so suitable for computer simulations at $\Delta L \to 0$, because as we will see, each term in Eq. (23) behaves as $O(1)$ in this limit, whereas $S \to 0$, as it can be seen from Eq. (6). Both terms in Eq. (22) are positive-definite. This property is much more suitable for numerical applications.

The OFM described briefly above may give relevant estimation for the PDF $P(L)$, when the rare enough fluctuation touches many particles of the system. This situation takes place for negative ΔL, when its absolute value is significantly larger than $\sqrt{\mathrm{var}\, L}$. More exact criteria will be considered in Sec. III, when we will obtain our asymptotic expression for $S(L)$.

For sufficiently large positive ΔL the situation is quite different, and our evaluation of the PDF $P(L)$ for this case cannot be obtained in the frame of the OFM, because of a completely different scaling with N.

III. NEGATIVE ATYPICAL FLUCTUATIONS OF L

We try in this section to obtain a solution of the mathematical problem we set in previous Sec. II for sufficiently small negative ΔL, $|\Delta L| \ll 1$. Our main obstacle to do this is how to determine $\lambda(t)$ that minimizes the action functional $S[\lambda(t)]$. However, we are able to obtain a solution to the problem within a quite reasonable class of functions $\lambda(t)$ that may give negative ΔL tending to 0. We obtain such solutions numerically as well as analytically. The latter one concerns only a leading order of the solution at $\Delta L \to 0$. Such an approach would appear to give only an upper boundary for $S(L)$. However, our final results show that $S(L)/\Delta L^2 \to 0$ at $\Delta L \to 0^-$. Such behavior is possible only for quite specific forms of $\lambda(t)$, so that an optimal $\lambda(t)$ is determined almost uniquely at $(-t) \ll 1$ as well as a leading term of $S(L)$ asymptotics at $\Delta L \to 0^-$.

We introduce in Sec. III A a one parametric set of particular $\lambda(t)$ and investigate analytically and numerically such OFM solutions including calculation of the action at $\Delta L \to 0^-$. Then we explain in Sec. III B that the upper bound for the action obtained in this way at $\Delta L \to 0^-$ has the same leading order of the true action $S(L)$, calculated along optimal trajectories at $\Delta L \to 0^-$.

A. A particular choice for $\lambda(t)$

We consider in this section the following choice of one parametric set for $\lambda(t)$:

$$\lambda(-\infty < t < 0) = -\frac{\sqrt{t_\lambda}}{4} \times \begin{cases} 64 \times 3^{-3/2} \times e^{3/2+8(t-t_\lambda)} & \text{for} \quad t < -3/16 + t_\lambda, \\ (t_\lambda - t)^{-3/2} & \text{for} \quad -3/16 + t_\lambda < t < 0. \end{cases} \tag{24}$$

This set of $\lambda(t)$ has the single positive parameter t_λ: $0 < t_\lambda \ll 1$. The solution of the OFM problem (which, to remind the reader, is summarized in Appendix A) with such $\lambda(t)$ gives in particular the value of $L(0)$ that depends on t_λ. We will see that $L(0)$ depends monotonically on t_λ at small t_λ, and $L(0) \to \bar{\ell}_0^-$ at t_λ tending to 0. We will see also that leading order of the action (22) along the trajectories defined by such $\lambda(t)$ is determined by times $t_\lambda \ll (-t) \ll 1$ and corresponds to the expression

$$S(L(0)) = \frac{\pi}{4} \frac{\Delta L^2}{|\ln \Delta L^2|} + \cdots, \tag{25}$$

whereas the parts of the trajectories on the time intervals $0 < (-t) \lesssim t_\lambda$ and $1 \lesssim (-t) < \infty$ contribute only to the subleading term in Eq. (25) at $\Delta L \to 0^-$. We will see also in Sec. III B that introducing of a constant multiplier in Eq. (24) of the order of $O(1)$ at $\Delta L \to 0^-$ does not change the leading order in Eq. (25) and influences only the subleading order.

The most important part of the trial function $\lambda(t)$ corresponds to the second line in Eq. (24). Its possible form for optimization of the action will be considered in detail in Sec. III B. In this section we treat it as a trial function. The form of the first line in (24) is chosen more or less arbitrarily. We demand only a smooth matching to the second line and exponential decay of λ at $t \to -\infty$. The coefficient k in the exponent e^{kt} is chosen so that it is equal to the first decaying mode of the linearized Eq. (16) at $t \to -\infty$.

The OFM problem is completely symmetric against the mirror mapping $x \leftrightarrow -x$. Hence, it is quite natural to investigate only symmetric solutions. Only such a kind of solution will be considered below. We may note additionally that Eq. (16) for p, considered in the backward direction in time t, with the "initial" condition (16) does not depend at all on q at given $L(t)$. We believe that the latter problem has only a symmetric solution, obeying (14). We may recall that requirements of obeying Eq. (14) demands a specific choice for Λ.

1. *Analytic self-similar solutions*

We consider in this subsection an approximate analytic solution of the problem with $\lambda(t)$ defined in Eq. (24) under condition that

$$t_\lambda \ll (-t) \ll 1. \tag{26}$$

In this case we may write instead of Eq. (24)

$$\lambda(t) = -\frac{1}{4} \frac{\sqrt{t_\lambda}}{(t_\lambda - t)^{3/2}}, \tag{27}$$

and we may hope to find an analytic solution of our problem, at least at times (26). In the regime (26), we could neglect t_λ in the denominator Eq. (27) and below in comparison to $(-t)$. However, we leave it in this and analogous positions for clarity.

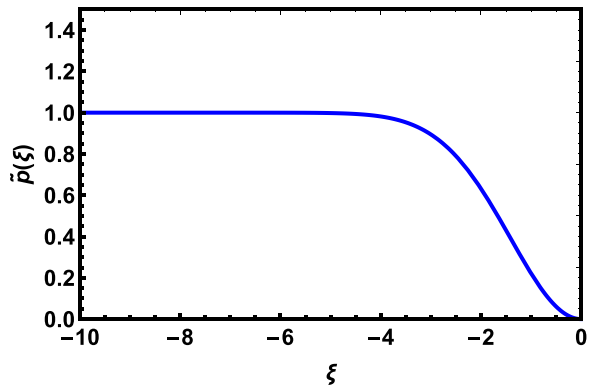

FIG. 2. Shown is $\tilde{p}(\xi)$ defined in Eq. (34) vs ξ.

We will see that the solutions are composed of two parts. At $L(t) - x \gg \sqrt{-t}$, the solution is simple and very smooth. Such interval of the x space we denote as $\bar{\Omega}$. At $0 < L(t) - x \lesssim \sqrt{-t}$, there is a somewhat nontrivial boundary layer. We will construct this part of the solution at the interval Ω, corresponding to the condition: $0 < L(t) - x \ll 1$. We approximate the solution at Ω by a self-similar solution, which will be described below. It is important that the domains $\bar{\Omega}$ and Ω are overlapping with each other at the interval $\sqrt{-t} \lesssim L(t) - x \ll 1$.

We will see below that

$$t\dot{L}(t) \ll \sqrt{-t} \tag{28}$$

for the solution defined by Eq. (27) under the condition (26). We assume this strong inequality for now, and justify it *a posteriori*. The inequality (28) means in particular that the edge displacement $\bar{\ell}_0 - L(t)$ is much less than the width of the boundary layer, where $\bar{\ell}_0 - x \sim \sqrt{-t}$.

Equation (16) can be rewritten in the domain $\bar{\Omega}$ as

$$\partial_t p = -\lambda(t). \tag{29}$$

Hence we have the following solution for $p(x,t)$ in this domain:

$$p(x,t) = p(0,t) = -\int_{-\infty}^{t} \lambda(t)\, dt = \frac{1}{2}\sqrt{\frac{t_\lambda}{t_\lambda - t}}. \tag{30}$$

Thus,

$$\Lambda \simeq \frac{1}{2}. \tag{31}$$

Taking in mind the strong inequality (28), Eq. (16) together with the boundary condition at the swarm edge can be rewritten in the domain Ω as

$$\partial_t p = -\partial_x^2 p - \lambda(t), \quad p(L(t),t) = 0. \tag{32}$$

Hence

$$p(x,t) \simeq \frac{1}{2}\sqrt{\frac{t_\lambda}{t_\lambda - t}}\left[1 - \exp\left(-\frac{(x - L(t))^2}{4(t_\lambda - t)}\right)\right] \tag{33}$$

for $x \in \Omega$. The function

$$\tilde{p}(\xi) = 2\sqrt{\frac{t_\lambda - t}{t_\lambda}}\, p(\xi\sqrt{t_\lambda - t} + L(t), t) = 1 - e^{-\xi^2/4} \tag{34}$$

is shown in Fig. 2. We see that the approximate solution inside the domain Ω has a self-similar form. The function $\tilde{p}(\xi)$ represents this self-similarity.

Introducing $\tilde{q}_0(x,t)$ in the domain $\bar{\Omega}$ by the following definition:

$$q(x,t) = U(x) + \tilde{q}_0(x,t), \tag{35}$$

we obtain the following equation for $\tilde{q}_0(x,t)$ inside the domain $\bar{\Omega}$ from Eq. (15):

$$\partial_t \tilde{q}_0 = pU(x) = \frac{1}{2}\sqrt{\frac{t_\lambda}{t_\lambda - t}}U(x). \tag{36}$$

This equation may give only that $\tilde{q}_0(x,t) \sim \sqrt{t_\lambda}U(x)$ and it is determined by the time $(-t) \sim 1$ that is outside the accuracy of the approximate solution considered in this section. In any case $\tilde{q}_0(x,t)/U(x) \sim \sqrt{t_\lambda} \ll 1$ in the domain $\bar{\Omega}$ at $t_\lambda \ll 1$. Inside the domain Ω we may use the following ansatz for q:

$$q(x,t) \simeq \frac{L(t) - x}{2} + \tilde{q}\left(\frac{x - L(t)}{\sqrt{t_\lambda - t}}\right)\sqrt{t_\lambda}, \tag{37}$$

where

$$\dot{L}(t) = -\frac{\sqrt{t_\lambda}}{t_\lambda - t}\, f \quad (f = \text{const} \sim 1). \tag{38}$$

The boundary condition (13) and the conservation law (10) give the following boundary conditions for $\tilde{q}$:

$$\tilde{q}(0) = 0, \tag{39}$$

$$\begin{aligned} -2\left(\frac{\partial \tilde{q}}{\partial x}\right)_{x=L(t)} &= -2\sqrt{\frac{t_\lambda}{t_\lambda - t}}\,\tilde{q}'(0) \\ &= \int_{-L(t)}^{L(t)} q(x,t)p(x,t)\, dx \\ &\simeq p(0,t) = \frac{1}{2}\sqrt{\frac{t_\lambda}{t_\lambda - t}}. \end{aligned} \tag{40}$$

Hence,

$$\tilde{q}'(0) = -\tfrac{1}{4}. \tag{41}$$

Substituting the ansatz (37)–(38) into Eq. (15), we obtain the following approximate equation for $\tilde{q}$:

$$\frac{\dot{L}(t)}{2} + \partial_t \tilde{q} = \partial_x^2 \tilde{q} - \partial_x[(L(t) - x)\,\partial_x p]. \tag{42}$$

This equation should be considered as linear relative to all perturbations of the equilibrium state. Using the expression (33) for p inside the domain Ω, we obtain that the function $\tilde{q}(\xi)$ obeys the following ODE:

$$-\frac{f}{2} + \frac{\xi}{2}\tilde{q}' = \tilde{q}'' + \frac{1}{4}(\xi^2 e^{-\xi^2/4})'. \tag{43}$$

Its unique solution obeying the condition (39) as well as a reasonable condition at $\xi \to -\infty$ can be presented as

$$\begin{aligned} \tilde{q}(\xi) = -\frac{f}{4}\left[\xi^2\, {}_2F_2\left(\{1,1\}, \left\{\frac{3}{2}, 2\right\}, \frac{\xi^2}{4}\right) + 2\pi\,\text{erfi}\left(\frac{\xi}{2}\right)\right] \\ + \frac{\xi}{4}e^{-\xi^2/4}. \end{aligned} \tag{44}$$

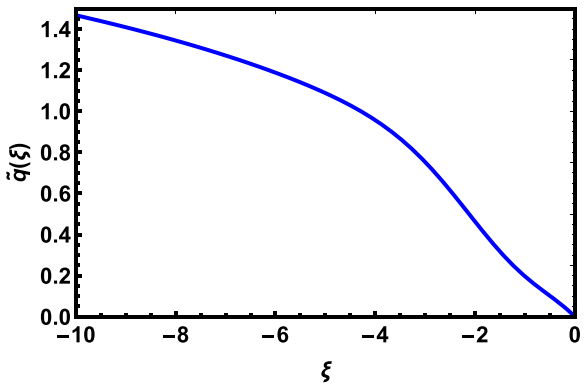

FIG. 3. Shown is $\tilde{q}(\xi)$ defined in Eq. (46) vs ξ.

Here ${}_mF_n(\cdots)$ and erfi$(\cdot)$ are the generalized hypergeometric function and the imaginary error function, respectively [27]. We have

$$\tilde{q}(\xi \to 0) = -\frac{f\sqrt{\pi}}{2}\xi + \frac{1}{4}\xi. \tag{45}$$

This equation together with the boundary condition (41), coming from conservation of total number of bees, give

$$f = \frac{1}{\sqrt{\pi}}.$$

Plugging this into Eq. (44), we obtain

$$\tilde{q}(\xi) = -\frac{1}{4\sqrt{\pi}}\left[\xi^2\,{}_2F_2\left(\{1,1\},\left\{\frac{3}{2},2\right\},\frac{\xi^2}{4}\right) + 2\pi\,\mathrm{erfi}\left(\frac{\xi}{2}\right)\right] + \frac{\xi}{4}e^{-\xi^2/4} \tag{46}$$

and

$$\dot{L}(t) = -\frac{\sqrt{t_\lambda/\pi}}{t_\lambda - t}. \tag{47}$$

The function $\tilde{q}(\xi)$ is shown in Fig. 3. At $\xi \to -\infty$, it behaves as

$$\tilde{q}(\xi) \to \frac{1}{2\sqrt{\pi}}\left(\ln \xi^2 + \gamma_E\right) \quad (\xi \to -\infty), \tag{48}$$

where $\gamma_E = 0.577\ldots$ is the Euler constant.

Thus, Eqs. (30), (33), (35)–(37), (46), and (47) give a complete description of our solution at $t_\lambda \to 0$ and under the condition (26). It obeys also the condition (28) that was used implicitly several times during this derivation.

2. Calculation of the action for the analytic solution

Equation (22) gives the following expression for the action rate $\dot{S}$ at $t_\lambda \ll (-t) \ll 1$:

$$\dot{S} = \frac{1}{2}\int_{-L(t)}^{L(t)} qp^2\,dx + \int_{-L(t)}^{L(t)} q(\partial_x p)^2\,dx, \tag{49}$$

because of the condition $p \ll 1$ during this period. The main contribution to the first integral comes from the domain $\bar{\Omega}$. Thus, it can be calculated as

$$\dot{S}_1 = \frac{1}{2}\int_{\bar{\Omega}} qp^2\,dx \simeq \frac{p^2(0,t)}{2}\int_{-\bar{\ell}_0}^{\bar{\ell}_0} U(x)\,dx = \frac{1}{8}\frac{t_\lambda}{t_\lambda - t}. \tag{50}$$

The main contribution to the second integral comes from the domain Ω:

$$\dot{S}_2 = \int_\Omega qp_x^2\,dx \simeq 2\int_0^{L(t)} \frac{L(t)-x}{2}\frac{t_\lambda}{4(t_\lambda - t)}\frac{[x-L(t)]^2}{4(t_\lambda - t)^2} \times \exp\left(-\frac{[x-L(t)]^2}{2(t_\lambda - t)}\right)dx. \tag{51}$$

Making here the substitution $[L(t)-x]/\sqrt{t_\lambda - t} = u$, we obtain

$$\dot{S}_2 \simeq \frac{t_\lambda}{16(t_\lambda - t)}\int_0^\infty u^3\,e^{-u^2/2}\,du = \frac{t_\lambda}{8(t_\lambda - t)}. \tag{52}$$

Combining both contributions to the action rate we obtain

$$\dot{S} = \dot{S}_1 + \dot{S}_2 = \frac{t_\lambda}{4(t_\lambda - t)}. \tag{53}$$

Thus we have expressions for $\dot{L}$ and $\dot{S}$ for our solution at $1 \ll -t \ll t_\lambda$; see Eqs. (47) and (53). We see that the total edge displacement ΔL as well the action S diverge at $t_\lambda - t \to 0$ and $\to \infty$ if we extend the expressions (47) and (53) outside their domain of applicability, $1 \ll -t \ll t_\lambda$. It is a key point of the OFM theory for this system at $\Delta L \to 0^-$. This property allows us to make integration over time interval $t \in (-1 + t_\lambda, 0)$ to get approximate evaluation of the whole action S and the whole edge displacement ΔL. The times $-t \gtrsim 1$ and $-t \lesssim t_\lambda$ give some contributions to these values that can be estimated as $\sim\sqrt{t_\lambda}$ and $\sim t_\lambda$, respectively. They can be neglected in the leading order for ΔL and S due to the "divergences" mentioned above. This assumption will be confirmed in Sec. III A 3 by a direct simulation of our whole problem. As a result, we have at $t_\lambda \to 0$

$$\Delta L = \sqrt{\frac{t_\lambda}{\pi}}\left[\ln t_\lambda + O(1)\right] \tag{54}$$

and

$$S = \frac{t_\lambda}{4}\left[\ln\frac{1}{t_\lambda} + O(1)\right]. \tag{55}$$

These two equations give the following relationship:

$$S\frac{|\ln \Delta L^2|}{\Delta L^2} = \frac{\pi}{4}\left[1 - 2\frac{\ln\ln\frac{1}{t_\lambda}}{\ln\frac{1}{t_\lambda}} + O\left(\frac{1}{\ln\frac{1}{t_\lambda}}\right)\right]. \tag{56}$$

For $t_\lambda \to 0$ (and hence, $\Delta L \to 0^-$) we obtain from the latter equation

$$S = \frac{\pi}{4}\frac{\Delta L^2}{|\ln \Delta L^2|} + \cdots \qquad (\Delta L \to 0^-). \tag{57}$$

This is our main result for $\lambda(t)$ given by Eq. (27) at times $1 \gg -t \gg t_\lambda$.

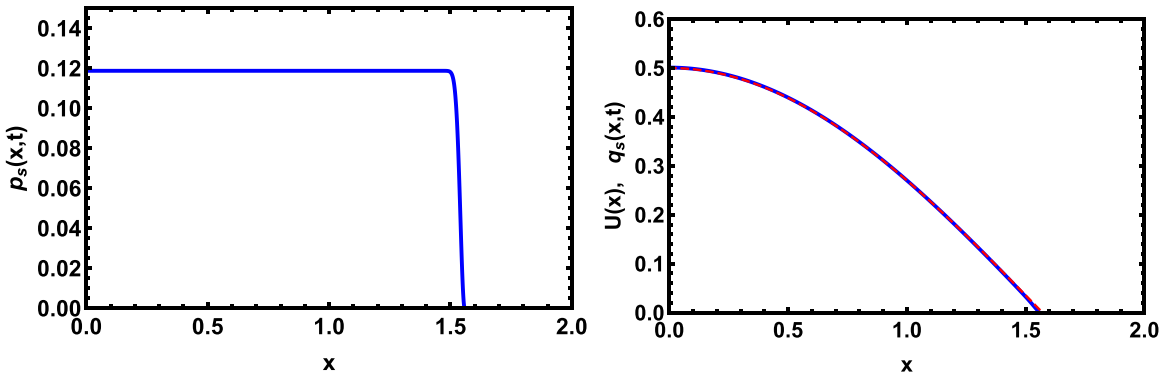

FIG. 4. Numerical solution of the OFM problem with $t_\lambda = 10^{-5}$ at $t = -15.7\,t_\lambda$. The solution in the bulk, in the domain $\bar{\Omega}$ is shown here. The left panel shows $p_s(x,t)$. Compare it with Eq. (30), which gives $p(x \in \bar{\Omega}, t) \simeq 0.122$ at this time. The right panel shows $q_s(x,t)$ by the solid (blue) line and $U(x)$ by the red (dashed) line; see Eq. (35). The difference between the latter two lines is almost invisible, excluding the region near $x = \bar{\ell}_0$ (the domain Ω)

3. *Numerical solution for the chosen* $\lambda(t)$

We numerically solve the OFM problem (summarized in Appendix A) at known $\lambda(t)$, given by Eq. (24). We replace the boundary condition (14) at infinite past on the boundary condition at finite time $t = -T$:

$$q(x,-T) = U(x), \quad p(x,-T) = 0, \tag{58}$$

where $T > 0$ is sufficiently large to exclude influence of finiteness of T on our solutions. Rigorously speaking, we cannot demand $p(x,-T) = 0$ for finite T. Actually, we replace the second condition in (58) by demanding that

$$p(0,-T) = 0. \tag{59}$$

This condition can be fulfilled at a specific value of Λ as can be seen from the set of equations (16), (21), and (58). The latter value is actually an eigenvalue of the problem, that depends on $\lambda(t)$. To be sure that our choice of T is large enough to approximate well the solution of the original problem (with $T \to \infty$), we calculate for this specific value of Λ the integral $\int_{-\bar{\ell}_0}^{\bar{\ell}_0} p^2(x,-T)\,dx$. We checked that this integral would be sufficiently small for our choice of T.

We solve this boundary value problem with the iteration procedure, originating from [28]. The parameter Λ plays a role of an eigenvalue. Each step of the iteration consists of two substeps: (1) forward and (2) backward. Equation (15) for q is solved forward in time with the boundary condition (58) treated as an initial condition. We use at this substep the function p, obtained during the previous iteration step. Then Eq. (16) is solved backward in time for p using the boundary condition (21) as an initial condition. Our present problem has an unusual feature. It is a free boundary problem with unknown in advance $L(t)$. We calculate $L(t)$ in the forward substep of the iteration procedure using the condition (10) simultaneously with solving Eq. (15). Details of this procedure are given in Appendix B. During the backward substep of the iteration we used $L(t)$ obtained at the previous forward substep.

This method allows us to find the solution with given $\lambda(t)$ and Λ. It does not satisfy yet the condition (59) for p. Using the method described in the previous paragraph, we apply a shooting procedure to find such value of Λ, which corresponds to a solution obeying Eq. (59).

Important details providing the numerical solution of the OFM problem at known $\lambda(t)$ are given in Appendix B. We applied this method for the one-parametric set (24) of functions $\lambda(t)$ with $t_\lambda = 0.1$, 0.02, 10^{-2}, 10^{-3}, 10^{-4}, 10^{-5}, and 10^{-6}.

First of all, we compare the simulated $q_s(x,t)$ and $p_s(x,t)$ with the self-similar solution considered in Sec. III A 1 at small t_λ. We designate the simulated q and p by the subscript "s." Figures 4 and 5 show the numerical solution with $t_\lambda = 10^{-5}$ at $t = -15.7\,t_\lambda = 1.57 \times 10^{-4}$. Figure 4 shows the numerical solution in the bulk, in the domain $\bar{\Omega}$.

To compare the self-similar-like solution (in the domain Ω) to the simulations we may use the following expressions:

$$\tilde{q}_s(\xi,t) = \frac{1}{\sqrt{t_\lambda}} q_s[L(t) + \xi\sqrt{t_\lambda - t}, t] + \xi\sqrt{\frac{t_\lambda - t}{4t_\lambda}} \tag{60}$$

and

$$\tilde{p}_s(\xi,t) = \sqrt{\frac{4(t_\lambda - t)}{t_\lambda}}\, p_s[L(t) + \xi\sqrt{t_\lambda - t}, t]. \tag{61}$$

Compare these expressions with Eq. (37) and Eqs. (33) and (34), respectively. These expressions should coincide with the self-similar analytic solutions $\tilde{q}(\xi)$ and $\tilde{p}(\xi)$ of Sec. III A 1, respectively, at $1 \ll (-t) \ll t_\lambda$ and $t_\lambda \to 0$.

Comparison of $\tilde{p}_s(\xi,t)$ with theoretical $\tilde{p}(\xi)$ is presented in Fig. 5(a). The curve $\tilde{p}_s(\xi,t)$, presented there, is obtained from the simulation with $t_\lambda = 10^{-5}$ and $t = -15.7\,t_\lambda$. We use the expression (61) to calculate $\tilde{p}_s(\xi,t)$. Analogously, Fig. 5(b) shows comparison of $\tilde{q}_s(\xi,t)$ with the theoretical curve $\tilde{q}(\xi)$. The same simulated data but for $q_s(x,t)$ are used to calculate $\tilde{q}_s(\xi,t)$ in accordance with Eq. (60). We see that the correspondence between simulated and self-similar solutions is quite acceptable. We checked that the same statement is valid for all times from the interval $0.03 \gtrsim (-t) \gtrsim t_\lambda$ for sufficiently small t_λ (not shown). This means that indeed the self-similar solutions, considered in Sec. III A 1, correctly describe the intermediate asymptotic behavior of the full OFM solutions corresponding to the set of $\lambda(t)$, defined in Eq. (24), at $t_\lambda \to 0$.

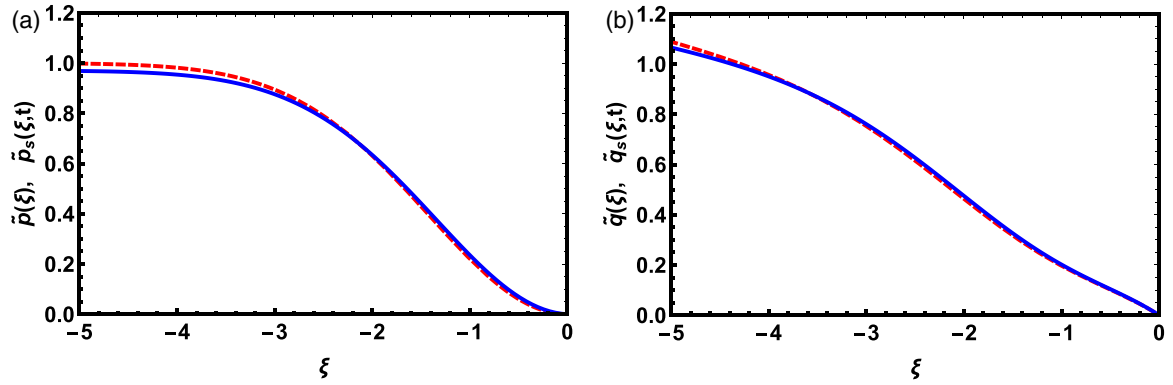

FIG. 5. Shown is a comparison of the (theoretical) self-similar and numerical solutions. The left panel shows the momentum in the domain Ω. The right panel shows the normalized bees' density q. The solid (blue) curves are obtained from numerical results for $t_\lambda = 10^{-5}$ and $t = -15.7\,t_\lambda$ in accordance to Eqs. (61) and (60), respectively. The dashed (red) lines are the self-similar solutions (33) and (46), respectively.

Now we proceed to analysis of the integral parameters of the numerical solutions, total action, S, and total edge displacement, ΔL. They depend now on t_λ only. Figures 6 and 7 show comparison of dependencies of normalized total displacements $\Delta L/\sqrt{t_\lambda}$ and normalized total actions S/t_λ on t_λ with fits based on Eqs. (54) and (55). To get self-similar theoretical results (54) and (55) we integrated the expressions (47) and (53) over t formally from $t = -1 + t_\lambda$ to $t = 0$. Keeping in mind an analytically uncertain contributions to these integrals from the regions $(-t) \gtrsim 1$ and $0 < (-t) \lesssim t_\lambda$, we may suppose the existence of analytically uncertain constant multipliers of the order of 1 under the logarithms. We add such multipliers to fit the simulated data. The blue lines in Figs. 6 and 7 correspond to a specific choice of these factors. Actually the blue line in Fig. 6 corresponds to the relationship

$$\Delta L = \sqrt{\frac{t_\lambda}{\pi}}\,\ln 3.65 t_\lambda. \tag{62}$$

Comparing it with Eq. (54), we may conclude that the numerical solutions confirm existence of the logarithm and even the coefficient $1/\sqrt{\pi}$ in Eq. (47), when $t_\lambda \ll 1$. At $t_\lambda \sim 10^{-6}$–10^{-5} the contribution of the multiplier 3.65 to the leading order becomes really small. Analogously, the blue line in Fig. 7 corresponds to the relationship

$$S = \frac{t_\lambda}{4}\,\ln\frac{0.061}{t_\lambda}. \tag{63}$$

It can be compared with Eq. (55). Although the subleading term determined by the factor 0.061 is relatively higher than the analogous correction in Eq. (63), nevertheless the leading order term dominates at $t_\lambda \sim 10^{-6}$–10^{-5}. Thus, the numerical solutions confirm the existence of the logarithm multiplier in the asymptotics (55) as well as the overall coefficient $1/4$ in it.

The dependence $S(\Delta L)$ defined parametrically by Eqs. (62) and (63) is plotted in Fig. 8. It shows also points obtained from results of the simulations. We see that subleading terms, caused by the approximate exclusion of t_λ from Eqs. (62) and (63) [or from Eqs. (54) and (55)], are well seen at our ΔL (or t_λ). To reveal this fact analytically we may consider Eq. (56). The third term in the right-hand side of this equation is of the same order of what would give subleading order terms in Eqs. (54) and (55). We see their relative contributions decay only logarithmically at $t_\lambda \to 0$. Nevertheless, the second term in the right-hand side of Eq. (56) is decaying even slower. We see that to reach the region where the subleading term would be about 10% of the leading term in this equation we should set $t_\lambda \lesssim 10^{-19}$.

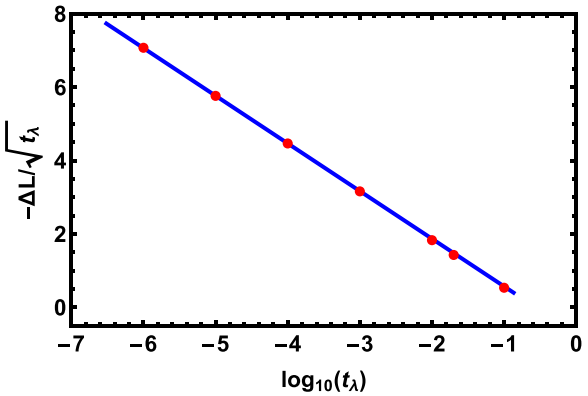

FIG. 6. Simulated relationship between the edge displacement ΔL and t_λ. The markers represent results of the simulations. The (blue) line shows the fit (62). See also Eq. (54).

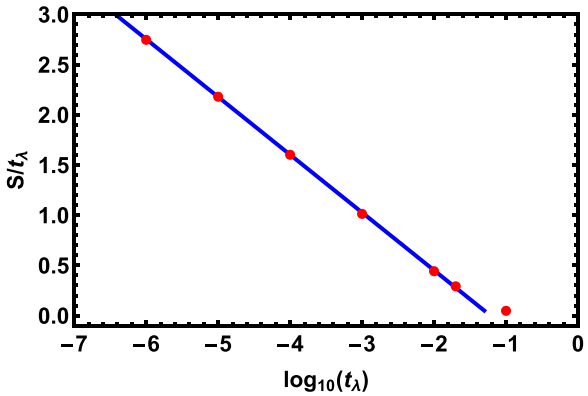

FIG. 7. Simulated relationship between the action S and t_λ. The markers represent results of the simulations. The (blue) line shows the fit (63). See also Eq. (55).

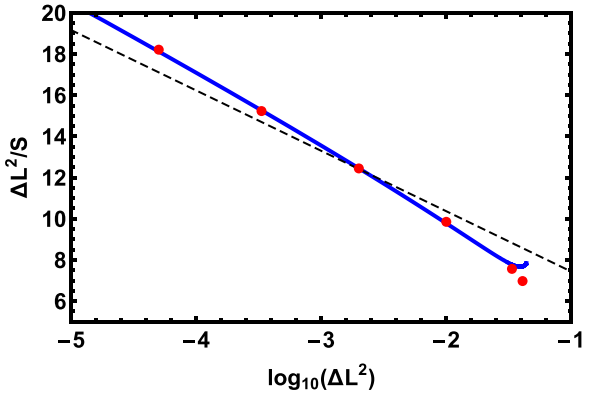

FIG. 8. The solid (blue) line is a curve defined parametrically by Eqs. (62) and (63). The markers are obtained from results of the numerical solutions. The dashed (black) line corresponds to $S = (\pi/4)\Delta L^2/|\ln(0.011\Delta L^2)|$. Existence of subleading terms, considered in the text, is seen apparently.

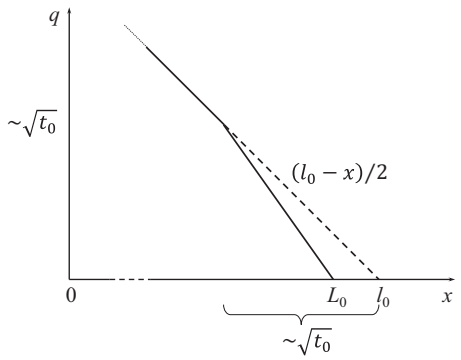

FIG. 9. Shown is a sketch for $q(x, 0)$ in the case of single time scale $\lambda(t)$, when $p(0, 0)$ and the timescale $t_0 \ll 1$. It corresponds to the solid line. The region $\bar{\ell}_0 - x \ll 1$ is shown only. The dashed line presents $U(x)$. The area between the dashed and solid lines can be estimated as $\sim(\bar{\ell}_0 - L_0)\sqrt{t_0}$.

Such values seems to us to be unreachable for our present numerical methods. Nevertheless, we may say that the simulations confirm surely the asymptotic behaviors (54) and (55) at $t_\lambda \to 0$ for the set (24) of the functions $\lambda(t)$.

Combining together all results of Secs. III A 1–III A 3, we may draw the following conclusions about the OFM solutions with $\lambda(t)$, defined by Eq. (24) and parameterized by t_λ, tending to 0:

(i) The main contributions to the displacement of the edge and to the action come from the time interval $t_\lambda \ll (-t) \ll 1$.

(ii) The OFM solutions at $t_\lambda \ll (-t) \ll 1$ can be well described by the self-similar solutions investigated in Secs. III A 1 and III A 2.

(iii) As a result, the action, S, on this set of solutions can be described by Eq. (57) at $\Delta L \to 0^-$.

(iv) Non-self-similar contributions to the displacement, ΔL, and to the action, S, influence only subleading terms in Eq. (57).

B. General remarks about the OFM solution

We explain in Sec. III A that the one parametric set of the functions $\lambda(t)$, determined by Eq. (24), gives the asymptotic relationship between the action, S, and the edge displacement, ΔL, presented by Eq. (57). Since this relationship corresponds to a particular choice of the set of the functions $\lambda(t)$, we may conclude that Eq. (57) gives only an upper bound for $S(L)$ at $\Delta L \to 0^-$. Nevertheless, we present in this section arguments in favor of the claim that the specific behavior of the functions $\lambda(t)$ from this set at $t_\lambda \ll (-t) \ll 1$, when t_λ tends to 0, provides the valid asymptotic leading term in this expression as a solution of the OFM problem, described in Sec. II. The particular form of $\lambda(t)$ outside the time interval $t_\lambda \ll (-t) \ll 1$ determines only subleading terms in Eq. (57), but not the leading term. The subleading terms are neglected by us in Eq. (6). A key point for such conclusion is that $S(L)/\Delta L^2$ tends to 0 at $\Delta L \to 0^-$. This property could be valid only for a quite specific choice of the set of the functions $\lambda(t)$, and our choice of $\lambda(t)$ in Sec. III A ensures such specific properties.

We start our way to the set (24) of the functions $\lambda(t)$ from several examples of trial functions that show us how to obtain

$$\frac{S(L)}{\Delta L^2} \to 0 \quad \text{at} \quad \Delta L \to 0^-. \tag{64}$$

1. The case of single timescale

Let us first consider functions $\lambda(t)$ that have only a single timescale, t_0. We focus on the behavior of $p(0, t)$ and do not specify exactly $\lambda(t)$ in Eq. (16) providing such $p(0, t)$. For $0 < (-t) < t_0$ we set some $p(0, t) \sim p_0 > 0$ and set that $p(0, t)$ [as well as $p(x, t)$] tends quickly to 0 for larger $(-t)$. We consider below several combinations of t_0 and p_0 determined by strong inequalities.

The case of $t_0 \gg 1$: In this case we may use results of Ref. [3], devoted to persistent fluctuations in the Brownian bees model. We obtain that

$$S(L) \sim \Delta L^2\, t_0$$

for such trial functions. We may conclude that we should set t_0 as small as possible, while $t_0 \gg 1$, and that even for smallest possible $t_0 \sim 1$, we have $S \sim \Delta L^2$. The latter estimation is much higher than in Eq. (57) and does not obey the condition (64).

Considering the case of $t_0 \ll 1$, we separate it into two limiting subcases: (1) $p_0 \ll 1$ and (2) $p_0 \gg 1$.

The case of $t_0 \ll 1$ and $p_0 \ll 1$: We begin from case (1), when $p_0 \ll 1$. We will see that in this case absolute value of the edge displacement $\Delta L = L_0 - \bar{\ell}_0$ is much less than the width of the diffusion boundary layer, which can be estimated as $\sqrt{t_0}$. This boundary layer corresponds actually to the domain Ω introduced above. In this case the density distribution in Ω is similar to a quasiequilibrium distribution, which is adjusted to a new position of the swarm edge; see Fig. 9. The fields p and q outside this boundary layer (that corresponds actually to the domain $\bar{\Omega}$ introduced above) are not affected by the diffusion process during the time, when $(-t) \sim t_0$, besides a small increasing of q in this domain due to positive p. As a result, $p(x, t)$ is constant in space in the domain $\bar{\Omega}$. The total normalized number of particles will be almost the same as

in the equilibrium with a small excess $\Delta Q = \int_{\bar{\Omega}} (q - U)\, dx$, which can be estimated as $\Delta Q \sim p_0 t_0$. This excess in the bulk (in the domain $\bar{\Omega}$) should be compensated by a lack of particles in the domain Ω. See for clarification Fig 9. The lack ΔQ_e can be estimated as an area between the dashed and solid lines in Fig. 9. The former one represents initial equilibrium, $U(x)$ close to the edge, whereas the latter one represents perturbed $q(x, 0)$ close to the edge. This area can be estimated as $|\Delta L|\sqrt{t_0}$. Hence, $\Delta Q_e \sim |\Delta L|\sqrt{t_0}$. Owing to conservation of total number of particles, we should demand at least $\Delta Q \sim \Delta Q_e$, and, hence $\Delta L\sqrt{t_0} \sim -p_0 t_0$. As a result, we have the following estimation of ΔL in this case:

$$\Delta L \sim -p_0\sqrt{t_0}. \tag{65}$$

This estimations confirms our preliminary assumption that $|\Delta L| \ll \sqrt{t_0}$ in this case.

Let us estimate now the action for the case $p_0 \ll 1$ and $t_0 \ll 1$. Both contributions to the action in Eq. (22) are determined by the time interval $(-t) \sim t_0$. The first contribution is determined by the domain $\bar{\Omega}$, whereas the second one by the contribution from the diffusion boundary layer. It appears that the both contributions can be estimated as $p_0^2 t_0$. Hence,

$$S \sim p_0^2 t_0. \tag{66}$$

Combining Eqs. (65) and (66), we obtain the following estimation for the action S:

$$S \sim \Delta L^2. \tag{67}$$

First of all, we note that this action at $\Delta L \to 0$ does not obey the condition (64). We may note also that the action do not depend on t_0 or p_0 but only on their combination appearing in Eq. (65). This fact will be important below.

The case of $t_0 \ll 1$ *and* $p_0 \gg 1$*:* This case differs from the previous one in two points. The additional to the equilibrium normalized number of particles begotten during the period $(-t) \sim t_0$ can be estimated now as $\Delta Q \sim e^{p_0} t_0$, whereas the additional lack of particles near the edge can be estimated now as $\Delta Q_e \sim \Delta L^2$. The latter estimation comes from a reasonable assumption that the perturbation of the slope of $q(x, 0)$ in the boundary layer is of the order of the slope in the equilibrium. Thus, due to conservation law ($\Delta Q \sim \Delta Q_e$), we have

$$\Delta L^2 \sim e^{p_0} t_0. \tag{68}$$

Only the first term in Eq. (22) gives considerable contribution to the action. As a result we have

$$S \sim p_0 e^{p_0} t_0. \tag{69}$$

Combining these two equations we obtain for the present case

$$S \sim p_0 \Delta L^2 \quad (p_0 \gg 1). \tag{70}$$

We see that the lowest possible action for $p_0 \gtrsim 1$ takes place at $p_0 \sim 1$. Again even in the latter case ($p_0 \sim 1$) this action at $\Delta L \to 0$ is much higher than the action (57) for particular solutions, considered in Sec. III A.

We may draw the following general conclusion for the cases of a single timescale trial functions $\lambda(t)$. Such trial functions give that $S \sim \Delta L^2$ or higher. In any case the action becomes much higher than the action (57) at $\Delta L \to 0^-$ for particular solutions, considered in Sec. III A.

2. Multiscale in time trial functions

Before turning to power-law form of trial functions $\lambda(t)$, which could be a candidate for the multiscale in time trial functions, we consider in more details a degeneracy revealed when we considered the case t_0 and $p_0 \ll 1$ in Sec. III B 1. We saw there that any time interval $(-t) \sim t_0$ of length t_0 give the same contributions to ΔL and S, if

$$p_0 \propto \frac{1}{\sqrt{t_0}} \quad \text{or} \quad \lambda \propto -\frac{1}{t_0^{3/2}}. \tag{71}$$

As a result, we may assume that if

$$\lambda(t) = -\frac{p_\lambda t_\lambda^{1/2}}{(t_\lambda - t)^{3/2}} \quad \text{or} \quad p(0, t) \sim p_\lambda \sqrt{\frac{t_\lambda}{t_\lambda - t}} \tag{72}$$

at the interval

$$t_\lambda \ll (-t) \ll 1 \tag{73}$$

when $p_\lambda \lesssim 1$ and $t_\lambda \ll 1$, then each octave in $(-t)$ give the same contribution to ΔL and S. This contribution can be estimated in accordance to Eqs. (65) and (66) as $\delta\, \Delta L \sim -p_\lambda\sqrt{t_\lambda}$ and $\delta S \sim p_\lambda^2 t_\lambda$, respectively, regardless of t belonging the interval (73). The number of such octaves can be estimated as $\ln t_\lambda^{-1}$. Hence the total edge displacement and the total action can be estimated as $\Delta L \sim -p_\lambda\sqrt{t_\lambda} \ln t_\lambda^{-1}$ and $S \sim p_\lambda^2 t_\lambda \ln t_\lambda^{-1}$, respectively. Such relationships lead to $S \sim \Delta L^2/|\ln \Delta L^2|$. This action is much less than for the trial functions considered in Sec. III B 1 and obeys the condition (64). Such rough a estimation cannot give the correct overall numerical factor on the order of one in the latter expression. However, this consideration gives some insight into the origin of much smaller actions for multiscale time trial functions. We may see that power laws in Eq. (72) are actually quite similar with what we set in Eqs. (24) and (27).

A power-law trial function for $\lambda(t)$*:* We see that power-law functions for $\lambda(t)$ could lead to the condition (64). We consider here the following general power-law trial functions for $\lambda(t)$:

$$\lambda(t) = -\frac{p_\lambda t_\lambda^{\alpha-1}}{(t_\lambda - t)^\alpha}. \tag{74}$$

We consider such solutions of the OFM equations at the time interval (73), assuming $t_\lambda \ll 1$ and $p_\lambda \lesssim 1$. We assume that $\lambda(t)$ tends quickly to 0 for $(-t) \gtrsim 1$, and $\lambda(t) \sim -p_\lambda/\sqrt{t_\lambda}$. Then the solution for $p(x, t)$ in the domain $\bar{\Omega}$ becomes in accordance to Eq. (16) as follows:

$$p(x, t)|_{\bar{\Omega}} \sim \frac{p_\lambda t_\lambda^{\alpha-1}}{(t_\lambda - t)^{\alpha-1}}. \tag{75}$$

The solution for $q(x, t)$ inside the domain Ω can be treated as previously in the case of $p(0, 0) \ll 1$; see Fig. 9. However, we should make obvious redesignations: $L_0 - \bar{\ell}_0 \to t\dot{L}(t)$, and $t_0 \to (-t)$. Then we obtain analogously to Eq. (65)

$$t\dot{L}(t) \sim p(0, t)\sqrt{-t} \tag{76}$$

or

$$\dot{L}(t) \sim -\frac{p(0, t)}{\sqrt{-t}} \sim -\frac{p_\lambda t_\lambda^{\alpha-1}}{(t_\lambda - t)^{\alpha-1/2}}. \tag{77}$$

The calculation of $\dot{S}$ is quite similar to obtaining of Eq. (66) before multiplying $\dot{S}$ in Eq. (66) on t_0. Thus, we have

$$\dot{S}(t) \sim p(0,t)^2 \sim \frac{p_\lambda^2 t_\lambda^{2\alpha-2}}{(t_\lambda - t)^{2\alpha-2}}. \tag{78}$$

To get the total edge displacement, ΔL and the total action, S, determined by the time interval $t \in (-1+t_\lambda, 0)$, we should integrate the expressions in Eqs. (77) and (78), respectively, over dt on this interval. These contributions to ΔL and S can be written as

$$\Delta L \sim -\frac{p_\lambda t_\lambda^{1/2}}{|2\alpha-3|}\left|t_\lambda^{\alpha-3/2}-1\right|, \tag{79}$$

$$S \sim \frac{p_\lambda^2 t_\lambda}{|2\alpha-3|}\left|t_\lambda^{2\alpha-3}-1\right|, \tag{80}$$

when $\alpha \neq 3/2$. For sufficiently small $|\alpha - 3/2|$ and t_λ contributions to ΔL and S from this interval become considerably higher than contributions from the regions, when $(-t) \gtrsim 1$ and $\lesssim t_\lambda$. Eliminating p_λ, we obtain from these equations

$$S \sim |2\alpha-3|\,\Delta L^2 \frac{\left|t_\lambda^{2\alpha-3}-1\right|}{\left(t_\lambda^{\alpha-3/2}-1\right)^2}. \tag{81}$$

Tending $t_\lambda \to 0$ we have $\Delta L \to 0$; and S can be expressed in this limit as

$$S \sim |2\alpha-3|\,\Delta L^2 \tag{82}$$

for sufficiently small $|2\alpha - 3|$.

We may conclude that the lowest action will take place at $\alpha \to 3/2$. For any finite $|\alpha - 3/2|$ and sufficiently small t_λ we may make S lower at $\Delta L \to 0^-$ by choosing lower $|\alpha - 3/2|$. It means that $\alpha = 3/2$ corresponds to the optimal $\lambda(t)$ in the form of Eq. (74), if we consider the leading-order behavior of S at $\Delta L \to 0^-$. Namely, this set of $\lambda(t)$ was considered analytically and numerically in Sec. III A.

Power-law trial function with slowly varying amplitude: It is interesting to introduce in Eq. (74) a very slowly variable factor at $\alpha = 3/2$, trying to diminish the leading order in the expressions (57) for the action. We assume that the change of the factor is relatively small if we multiply or divide the time t by 2. As a result, we present $\lambda(t)$ in the form

$$\lambda(t) = -\frac{t_\lambda^{1/2}}{(t_\lambda - t)^{3/2}} F\left(\ln\frac{1}{|t|}, \ln\frac{1}{t_\lambda}\right). \tag{83}$$

We assume again that this expression is valid for $t_\lambda \ll (-t) \ll 1$. Contributions to action outside this interval again determines only subleading orders at $\Delta L \to 0^-$. When absolute value of partial derivative of the function F with respect to the first argument is much less than 1, then dependence of F on t can be treated adiabatically. Then repeating previous estimations we can write

$$\Delta L \sim -\sqrt{t_\lambda}\int_{t_\lambda}^1 F\left(\ln\frac{1}{|t|}, \ln\frac{1}{t_\lambda}\right)\frac{d|t|}{|t|} \tag{84}$$

and

$$S \sim t_\lambda \int_{t_\lambda}^1 F^2\left(\ln\frac{1}{|t|}, \ln\frac{1}{t_\lambda}\right)\frac{d|t|}{|t|}. \tag{85}$$

Hence

$$S \sim \Delta L^2 \frac{\int_{t_\lambda}^1 F^2\left(\ln\frac{1}{|t|}, \ln\frac{1}{\Delta\ell^2}\right)\frac{d|t|}{|t|}}{\left[\int_{t_\lambda}^1 F\left(\ln\frac{1}{|t|}, \ln\frac{1}{\Delta\ell^2}\right)\frac{d|t|}{|t|}\right]^2}. \tag{86}$$

Minimizing this expression at given ΔL, we obtain that optimal F has not to depend on $\ln|t|$:

$$F = \text{const} = p_\lambda. \tag{87}$$

As a result we may conclude that optimal $\lambda(t)$ has to have a form of Eq. (72) at $\Delta L \to 0^-$. The only question that should be solved is the question about the amplitude p_λ in Eq. (72).

A choice of the constant p_λ in Eq. (72): As a consequence of the arguments above, p_λ for the optimal $\lambda(t)$ cannot be much larger than 1. Thus we set straightly that $p_\lambda \lesssim 1$ in the optimum. For such p_λ we are able to make substitution $p_\lambda^2 t_\lambda$ instead of t_λ in the amplitude of $\lambda(t)$ in the definition (27) of Sec. III A 1, where we considered analytic solution of the OFM equations with $\lambda(t)$ defined in Eq. (27). Analogous substitutions in all further expressions in that section lead to the following slightly more general final results than in Sec. III A 1 [Eqs. (54) and (55)]:

$$\Delta L = p_\lambda\sqrt{\frac{t_\lambda}{\pi}}\left[\ln t_\lambda + O(1)\right], \tag{88}$$

$$S = \frac{p_\lambda^2 t_\lambda}{4}\left[\ln\frac{1}{t_\lambda} + O(1)\right]. \tag{89}$$

It is worth to remind once again that the residual terms, O in these equations are of the order of 1, and they are determined by by unknown behavior of $\lambda(t)$ at $(-t) \gtrsim 1$ and $\sim t_\lambda$ in the optimum. These equations give

$$S(L) = \frac{\pi}{4}\frac{\Delta L^2}{\ln(p_\lambda/\Delta L)^2} + \cdots \quad (\Delta L \to 0^-). \tag{90}$$

If $p_\lambda \sim 1$, then it can be skipped at all or transferred to the residual term. However, when $p_\lambda \ll 1$, it leads to an increase of the trial action. This means that the optimal $p_\lambda \sim 1$ and its exact value do not influence on the asymptotic behavior of S in the leading order. Our choice $p_\lambda = 1/4$ in Sec. III A follows this conclusion, and its concrete numerical value was chosen only for numerical convenience.

Final OFM result: Combining now the OFM results (88) and (89), we obtain similarly to obtaining of Eq. (56):

$$S(L) = \frac{\pi}{4}\frac{\Delta L^2}{|\ln\Delta L^2|}\left[1 - 2\frac{\ln|\ln\Delta L^2|}{|\ln\Delta L^2|} + O\left(\frac{1}{|\ln\Delta L^2|}\right)\right] \quad (\Delta L \to 0^-). \tag{91}$$

Our main statement is that this is the valid OFM result at $\Delta L \to 0^-$. The nonoptimized value of the overall factor $\sim O(1)$ in our trial function $\lambda(t)$, as well as its nonoptimized behavior at $(-t) \gtrsim 1$ and at $(-t) \sim t_\lambda$ may change only the $\sim O(1)$ coefficient before $\ln^{-1}(\Delta L)^{-2}$ in the residual term $O(\ln^{-1}(\Delta L)^{-2})$ that is of the order of 1. The order of this residual term is confirmed by the numerical simulations in Sec. III A 3.

The result [4] concerning variance of L for typical fluctuations means that $P(L)$ can be presented for such fluctuations

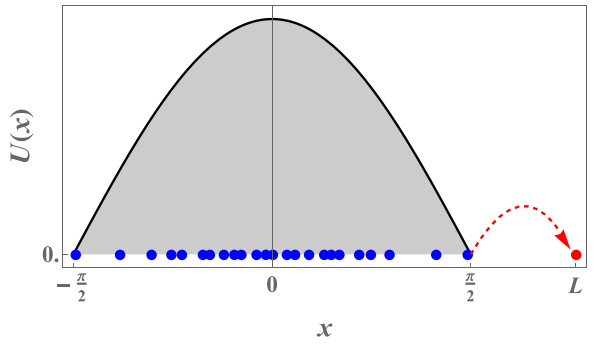

FIG. 10. Atypical positive fluctuations of ΔL are dominated by the "runaway particle" scenario, in which a single particle quickly travels from the edge support of $U(x)$, at $x = \pi/2$, to the position $x = L$, while the rest of the particles do not display any unusual behavior. During the creation of this fluctuation, the branching process is entirely suppressed.

as

$$-N^{-1} \ln P(L) \simeq \frac{\pi}{4} \frac{\Delta L^2}{\ln N}. \tag{92}$$

Our main result (6) followed from Eq. (91) coincides with Eq. (92) with the relative accuracy $\varepsilon \to 0$, when ΔL belongs for example the interval $\mathcal{L} = (-1/\sqrt{N^{1-\varepsilon}}, -1/\sqrt{N})$. For any small ε and sufficiently high N, $|\Delta L|$ varies on this interval $\mathcal{L}$ in many times. It means that the result (92) for typical fluctuations and our result (6) have a wide region near the point $\Delta L = \sqrt{\mathrm{var}\,(L)}$, where they coincide with a high accuracy. This fact strengths the reliability of both results.

IV. POSITIVE ATYPICAL FLUCTUATIONS OF L: SINGLE-PARTICLE APPROXIMATION

Fluctuations with an unusually large swarm radius, $L > \bar{\ell}_0$, turn out to behave entirely differently from the case $L < \bar{\ell}_0$ that we considered in the previous section. As we find below, the system trajectories that dominate the probability for observing some value $L > \bar{\ell}_0$ are those for which a single, runaway particle travels relatively quickly from $x = \bar{\ell}_0$ to $x = L$, whereas the other particles simply diffuse, and meanwhile the branching process is completely suppressed. This scenario is schematically depicted in Fig. 10.

The runaway particle scenario is similar in spirit to similar approaches in extreme-value statistics [24]. In particular, it is rather reminiscent of the "evaporation" scenario that describes the right tail of the statistics of the largest eigenvalue in many random matrix ensembles [29–33]. In fact, this approach was also recently employed to describe fluctuations of the size of a model that is not so different to the Brownian bees model, in which the branching and particle removal processes are replaced by stochastic resetting of the particles' positions to the origin [34].

Assuming this scenario of a single, runaway particle, the problem simplifies considerably. One can write down a very simple equation for the dynamics of the PDF $P_1(x,t)$ of the particle that is farthest from the origin, by neglecting the possibility that it will be overtaken by one of the other particles:

$$\partial_t P_1(x,t) = \partial_x^2 P_1(x,t) - N P_1(x,t) \quad (x - \bar{\ell}_0 > 0). \tag{93}$$

The two terms on the right-hand side of Eq. (93) describe diffusion of the furthest particle from the origin, and an effective "mortality" term that corresponds to branching of one of the other $N-1$ particles (we neglect here the difference between N and $N-1$ at $N \gg 1$). This equation is expected to be valid at $x - \bar{\ell}_0$ that is much larger than the scale of typical fluctuations, where it becomes very unlikely for the positions of the two furthest particles from the origin to cross each other. The steady-state solution of this equation is quite obvious $P_1(x) \propto e^{-x\sqrt{N}}$. As a result we find that positive fluctuations of L are described by

$$P(L) = P_1(L) \sim \exp(-\sqrt{N}\Delta L) \quad (\Delta L > 0). \tag{94}$$

A prefactor in this equation is determined by a crossover region, where one expects the PDF (92) for typical fluctuations to match somehow with Eq. (94). A full calculation of the prefactor is beyond the quantitative theory presented here. However, one may assume that this crossover takes place at ΔL for which the two formulas (92) and (94) predict probabilities that are of the same order. This happens at $\Delta L \sim \sqrt{\ln(N)\,\mathrm{var}\,(L)}$. In any case, Eq. (94) gives Eq. (7) from the Introduction.

Some insight is obtained by contrasting the results of this section with those of the previous one, which describe the two (very different) tails of the distribution $P(L)$. The scaling $-\ln P(L) \sim \sqrt{N}$ predicted by the runaway particle scenario of the present section, obviously predicts much larger probabilities than the scaling $-\ln P(L) \sim N$ predicted by the OFM of the previous section; see, e.g., (17). This confirms our assumption that, for $\Delta L > 0$, the runaway particle scenario dominates, whereas scenarios involving a large number of particles should not be taken into account as their contribution to $P(L)$ is negligible.

However, in analogy with the previous section, it would be nice to gain further information regarding the atypical $\Delta L > 0$ fluctuations, by characterizing the histories of the system that lead to a given $L > \bar{\ell}_0$. It turns out that this can be done quite simply, as follows. Let us consider a dynamical scenario in which, at time $t = -\tau$ (where $\tau \gg 1/N$ will be determined below) the system is in a state that is described by the density $U(x)$. Then, during the time interval $-\tau < t < 0$, (1) no branching events occur and (2) the rightmost particle travels from the edge of the support of $U(x)$, $x = \bar{\ell}_0$, arriving at $x = L$ at time $t = 0$. This scenario is shown schematically in Fig. 10.

What is the probability of this dynamical scenario? The probability for no branching events is (exactly) given by $e^{-N\tau}$. Conditioned on no branching events, the PDF of the position a particle initially at time $t = 0$ given that at time $t = -\tau$ it was at $x = \bar{\ell}_0$ is $e^{-(x-\bar{\ell}_0)^2/4\tau}/\sqrt{4\pi\tau}$. Therefore, the probability for this scenario, including arrival at $x = L$ at time $t = 0$, is

$$\sim e^{-N\tau - (\Delta L)^2/4\tau}, \tag{95}$$

up to a pre-exponential factor. It will be useful to rewrite this as

$$\sim e^{-\sqrt{N}\mathcal{F}(\tilde{\tau})}, \quad \mathcal{F}(\tilde{\tau}) = \tilde{\tau} + \frac{(\Delta L)^2}{4\tilde{\tau}}, \quad \tilde{\tau} = \sqrt{N}\,\tau. \tag{96}$$

The next step towards calculating the $\Delta L > 0$ tail of $P(L)$ is to integrate the probability (96) over $\tilde{\tau}$. Clearly, at $N \gg 1$ this integral is dominated by the saddle point, i.e., we obtain

$$P(L) \sim e^{-\sqrt{N}\mathcal{F}(\tilde{\tau}_*)}, \tag{97}$$

where $\tilde{\tau}_*$ is the minimizer of $\mathcal{F}(\tilde{\tau})$. This minimization is trivial; it yields $\tilde{\tau} = \Delta L/2$ so $\mathcal{F}(\tilde{\tau}) = \Delta L$, which, after plugging into (97), we obtain $P(L) \sim e^{-\sqrt{N}\Delta L}$ in perfect agreement with our earlier result (94).

V. SUMMARY AND DISCUSSION

We see that the PDF for the size L of the swarm in the frame of the "branching bees" model with $N \gg 1$ is quite asymmetric around its mean value $\bar{\ell}_0$, if we exclude at least the region of typical fluctuations of L determined by its variance (5) [4]. In particular, we find that unusually large positive fluctuations of L are far more likely than negative ones, as is evident from the very different scalings of the two distribution tails with N at $N \gg 1$. The atypically large negative fluctuations of L can be described by the OFM approach (6); and this PDF demonstrates the logarithmic anomaly that also appears in the variance (5) [4]. The OFM result matches smoothly with the Gaussian PDF determined by the variance. For atypically large positive fluctuations of L, their PDF (7) can be obtained with a single runaway particle approach. The region of crossover of the PDF between the latter one behavior and the Gaussian part of the PDF for typical fluctuations is an interesting goal for further investigations.

We saw that for $|\Delta L| \ll 1$ the fluctuations involve mainly a narrow layer of bees close to $\bar{\ell}_0$. As a result, we may assume that the principal results of this paper concerning $P(L)$ at $|\Delta L| \ll 1$ do not depend on dimension d of the space [up to a proper shift of the distribution $P(L)$, because $\bar{\ell}_0$ depends on d]. The Monte Carlo simulations in Ref. [4] for typical fluctuations and conclusions from them drawn there support this argument.

A model, which is similar to but slightly simpler than the Brownian bees model, was recently considered in Ref. [34]. In their "model B," the position of the particle farthest from the origin is stochastically reset to the origin (instead of being reset to the position of one of the other particles as in the Brownian bees model studied here). We believe that our main results, Eqs. (6) and (7), remain valid for the "model B" also (up to a proper shift, again because $\bar{\ell}_0$ is different). We draw such conclusion for negative ΔL from the fact that we were able to neglect the branching process for the self-similar solution in the domain Ω; see Eq. (36). For the positive ΔL this conclusion is even more obvious and derived actually in Ref. [34]. Moreover, we may assume that the entire PDF of L at $|\delta L| \ll 1$ and $N \to \infty$ for these two models are the same (up to the shift). Meanwhile, this statement is proven for the variance, var(L), in Ref. [34].

Several extensions of the model that we studied here could be investigated too. For example, one could consider higher spatial dimensions or the addition of external forces acting on the particles. Other modifications of the model are also possible, leading to nontrivial behavior; see e.g., [35,36].

ACKNOWLEDGMENTS

We are very grateful to B. Meerson and O. Vilk for useful discussions. The research of P.S. was supported by the project High Field Initiative (CZ.02.1.01/0.0/0.0/15_003/0000449) from the European Regional Development Fund.

APPENDIX A: FULL SET OF THE OFM EQUATIONS

The OFM equations of motion [see Eqs. (15) and (16)] for the 1D case are as follows:

$$\partial_t q = qe^p + \partial_x\,(\partial_x q - 2q\partial_x p), \tag{A1}$$

$$\partial_t p = -(e^p - 1) - \partial_x^2 p - (\partial_x p)^2 - \lambda(t). \tag{A2}$$

The full set of boundary conditions are as follows:

$$\int_{-L(t)}^{L(t)} q(x,t)\,dx \equiv 1, \tag{A3}$$

$$q(|x| = L(t), t) = p(|x| = L(t), t) = 0, \tag{A4}$$

$$q(x, t \to -\infty) = U(x), \quad p(x, t \to -\infty) = 0, \tag{A5}$$

$$p(x, 0) = \Lambda = \text{const} \quad \text{for } |x| < L(0). \tag{A6}$$

They are equivalent to Eqs. (10), (13), (14), and (21), respectively. The functions $q(x,t)$ and $p(x,t)$ are assumed to be defined in the domain $-\infty < t \leqslant 0$, $-L(t) \leqslant x \leqslant L(t)$. The function $U(x)$ is defined by Eq. (4) that means in particular that $L(-\infty) = \bar{\ell}_0$, defined below Eq. (4).

For any reasonable negative $\lambda(t)$, tending sufficiently fast to 0 at $t \to -\infty$, the above problem presumably has a unique solution, determining also Λ and $L(t)$. The solution determines also the action on the found trajectory:

$$S = \int_{-\infty}^{0} dt \int_{-L(t)}^{L(t)} dx\,[q(pe^p - e^p + 1) + q(\partial_x p)^2]. \tag{A7}$$

It determines the distribution of L as it is considered in Sec. II.

APPENDIX B: NUMERICAL METHOD

We describe here some details of the numerical analysis of the OFM problem in one dimension (summarized in Appendix A), where the constant Λ and functions $L(t)$, $q(x,t)$, $p(x,t)$ should be found, and $\lambda(t)$ is a given function; see Eq. (24). We introduce a spatial variable $y = x/L(t)$ ($|y| \leqslant 1$) to work with a stationary spatial grid. This change of variables causes Eqs. (15) and (16) to become

$$\partial_t q = y\frac{\dot{L}(t)}{L(t)}\partial_y q + \partial_y^2 q - \partial_y(\partial_y q - 2q\partial_y p) + qe^p, \tag{B1}$$

$$\partial_t p = y\frac{\dot{L}(t)}{L(t)}\partial_y p - \partial_y^2 p - (\partial_y p)^2 - (e^p - 1) - \lambda(t), \tag{B2}$$

respectively, while the initial and boundary conditions become

$$q(|y| = 1, t) = p(|y| = 1, t) = 0, \tag{B3}$$

$$q(y, t \to -\infty) = \frac{1}{2}\cos\left(\frac{\pi}{2}y\right),$$
$$p(y, t \to -\infty) = 0, \tag{B4}$$

$$p(y, 0) = \Lambda = \text{const}, \quad \text{for} \quad |y| < 1. \tag{B5}$$

In our numerical solutions, we replace time ∞ by finite time $T = 10$. The conservation condition (10) is

$$L(t)\int_{-1}^{1} q(y, t)\, dy = 1. \tag{B6}$$

As described in the main text, we solve Eqs. (B1) and (B2) using the back-and-forth Chernykh-Stepanov algorithm [28]. Every iteration of the algorithm consists of two steps. In the first step, we solve Eq. (B2) for $p(y, t)$ backwards in time from $t = 0$, using $q(y, t)$ and $L(t)$ from the previous iteration. In the second step, we solve Eq. (B1) forward in time for $q(y, t)$ using $p(y, t)$ that was found in the first step. During the forward step, we also compute $L(t)$ via Eq. (B6). We employ the implicit finite differences method to approximate Eqs. (B1) and (B2) and Newton's method to solve nonlinear algebraic equations to approximate p. A few iterations of the algorithm are sufficient for it to achieve convergence to a solution of Eqs. (B1) and (B2). One must, of course, specify some initial values in order to perform the first iteration of the algorithm. The choice usually does not have a strong effect on the convergence properties. We chose $\Lambda = \Lambda_1 \cong 1/2$, the mean field functions $q(0 < y < 1, -T \leqslant t < 0) = \cos[L(t)y]/2$ and $p(y, t < 0) = 0$, $p(y, 0) = \Lambda_1$, and $L(t) = \bar{\ell}_0$.

At the end of the iterations the functions $q(y, t, \Lambda_1)$, $p(y, t, \Lambda_1)$, and $L(t, \Lambda_1)$, in particular $p(y, -T, \Lambda_1)$ are known. The found function $p(y, -T, \Lambda_1)$ satisfies to condition $p(y, -\infty) = 0$ in Eq. (B4) for a certain value of Λ which we are to find. Since in the general case $p(y, -T, \Lambda_1)$ is not a constant, we employ a functional $F(\Lambda) = \int_{-1}^{1} p^2(y, -T)\, dy$. We seek now the value Λ_m that minimizes the functional F, which is calculated by the procedure described above. Notice that $F(\Lambda_m)$ is very close to zero for sufficiently small criteria ending the iterations. Finally L and S are computed on the solution through $L = L(t = 0)$ and Eq. (22), respectively.

We used nonhomogeneous time and space grids. The smallest time step τ_m at $t = 0$ depends on value of t_λ, $\tau_m \propto t_\lambda^2$ the value of the steps growth exponentially when $t \to -T$: $\tau_j = (1 + \delta\tau)\tau_{j+1}$, $t_j = t_{j-1} + \tau_j$. $j = 2, 3, \ldots, m$, $t_1 = -T$ and $t_m = 0$. For example $\tau_m = 10^{-13}$ and $\delta\tau = 0.01$ in calculation of version for $t_\lambda = 10^{-6}$. The space grid is exponential too, the minimal spacing is near $y = 1$: $h_2 \propto t_\lambda^{1/2}$, and the spacing increases with growth of y. For $t_\lambda = 10^{-6}$, we used $h_2 = 5 \times 10^{-5}$ and the increment $\delta h = 0.01$, $1 - y_{i+1} = (1 + \delta h)(1 - y_i)$, $i = 1, 2, 3, \ldots, n$, $y_1 = 1$, $y_n = 0$.

To illustrate the calculation of Λ, we give here the data when the shooting procedure was stopped for $t_\lambda = 10^{-6}$: $p(0, -T) \simeq -10^{-12}$, $\int_{-1}^{0} |p(y, -T)|\, dy \simeq 3 \times 10^{-12}$, $\int_{-1}^{0} p(y, -T)\cos(y)\, dy \simeq -3 \times 10^{-12}$.

It is important also that our numerical model has an steady-state mean field distribution which differs because of its discreetness from the continuous distribution $U(x)$, defined by Eq. (4). This difference really is very small. Nevertheless, we took it into account in the calculation of numerical ΔL to diminish the influence of numerical inaccuracies.

[1] J. Berestycki, É. Brunet, J. Nolen, and S. Penington, Ann. Probab. **50**, 2133 (2022).
[2] J. Berestycki, É. Brunet, J. Nolen, and S. Penington, Trans. Am. Math. Soc. **374**, 6269 (2021).
[3] B. Meerson and P. Sasorov, Phys. Rev. E **103**, 032140 (2021).
[4] M. Siboni, P. Sasorov, and B. Meerson, Phys. Rev. E **104**, 054131 (2021).
[5] H. P. McKean, Commun. Pure Appl. Math. **28**, 323 (1975).
[6] M. D. Bramson, Mem. Am. Math. Soc. **44**, 285 (1983).
[7] É. Brunet and B. Derrida, Europhys. Lett. **87**, 60010 (2009); J. Stat. Phys. **143**, 420 (2011).
[8] A. H. Mueller and S. Munier, Phys. Rev. E **90**, 042143 (2014).
[9] K. Ramola, S. N. Majumdar, and G. Schehr, Phys. Rev. Lett. **112**, 210602 (2014); Chaos Solitons Fractals **74**, 79 (2015); Phys. Rev. E **91**, 042131 (2015).
[10] B. Derrida, B. Meerson, and P. V. Sasorov, Phys. Rev. E **93**, 042139 (2016).
[11] G. Jona-Lasinio, C. Landim, and M. E. Vares, Probab. Theory Relat. Fields **97**, 339 (1993).
[12] G. Basile and G. Jona-Lasinio, Int. J. Mod. Phys. B **18**, 479 (2004).
[13] T. Bodineau and M. Lagouge, J. Stat. Phys. **139**, 201 (2010).
[14] P. I. Hurtado, A. Lasanta, and A. Prados, Phys. Rev. E **88**, 022110 (2013).
[15] B. Meerson, J. Stat. Mech. (2015) P05004.
[16] É. Brunet, B. Derrida, A. H. Mueller, and S. Munier, Europhys. Lett. **76**, 1 (2006).
[17] É. Brunet, B. Derrida, A. H. Mueller, and S. Munier, Phys. Rev. E **76**, 041104 (2007).
[18] V. Elgart and A. Kamenev, Phys. Rev. E **70**, 041106 (2004).
[19] B. Meerson and P. V. Sasorov, Phys. Rev. E **83**, 011129 (2011).
[20] B. Meerson, P. V. Sasorov, and Y. Kaplan, Phys. Rev. E **84**, 011147 (2011).
[21] L. Bertini, A. De Sole, D. Gabrielli, G. Jona-Lasinio, and C. Landim, Rev. Mod. Phys. **87**, 593 (2015).
[22] B. Meerson and P. V. Sasorov, Phys. Rev. E **84**, 030101(R) (2011).
[23] B. Meerson, A. Vilenkin, and P. V. Sasorov, Phys. Rev. E **87**, 012117 (2013).
[24] S. N. Majumdar, A. Pal, and G. Schehr, Phys. Rep. **840**, 1 (2020).

[25] In the left ($L < \ell$) distribution tail, $P(L) \sim \mathbb{P}\text{rob}(L < \ell)$ in the leading order, and the difference between them is only in the preexponential factor. Thus, we replace $P(L)$ by $\mathbb{P}\text{rob}(L < \ell)$ in Eq. (19) to reach Eq. (20).

[26] B. Derrida and A. Gerschenfeld, J. Stat. Phys. **137**, 978 (2009).
[27] F. W. J. Olver, D. W. Lozier, R. F. Boisvert, and C. W. Clark, *NIST Handbook of Mathematical Functions* (Cambridge University Press, Cambridge, 2010).
[28] A. I. Chernykh and M. G. Stepanov, Phys. Rev. E **64**, 026306 (2001).
[29] J. M. Kosterlitz, D. J. Thouless, and R. C. Jones, Phys. Rev. Lett. **36**, 1217 (1976).
[30] R. C. Jones, J. M. Kosterlitz, and D. J. Thouless, J. Phys. A: Math. Gen. **11**, L45 (1978).
[31] P. Facchi, U. Marzolino, G. Parisi, S. Pascazio, and A. Scardicchio, Phys. Rev. Lett. **101**, 050502 (2008).
[32] C. Nadal, S. N. Majumdar, and M. Vergassola, Phys. Rev. Lett. **104**, 110501 (2010).
[33] P. Facchi, G. Florio, G. Parisi, S. Pascazio, and K. Yuasa, Phys. Rev. A **87**, 052324 (2013).
[34] O. Vilk, M. Assaf, and B. Meerson, Phys. Rev. E **106**, 024117 (2022).
[35] L. Addario-Berry, J. Lin, and T. Tendron, Ann. Appl. Probab. **32**, 2504 (2022).
[36] P. L. Krapivsky, O. Vilk, and B. Meerson, Phys. Rev. E **106**, 034125 (2022).